

This is the accepted manuscript made available via CHORUS. The article has been published as:

# First-principles study of defect properties of zinc blende MgTe

Ji-Hui Yang, Shiyu Chen, Hongjun Xiang, X. G. Gong, and Su-Huai Wei

Phys. Rev. B **83**, 235208 — Published 14 June 2011

DOI: [10.1103/PhysRevB.83.235208](https://doi.org/10.1103/PhysRevB.83.235208)

# First-principles study of defect properties of zinc-blende MgTe

Ji-Hui Yang, Shiyu Chen, Hongjun Xiang?? and X. G. Gong  
*Key Laboratory for Computational Physical Sciences(MOST) and Surface  
Physics Laboratory, Fudan University, Shanghai-200433, P.R. China*

Su-Huai Wei  
*National Renewable Energy Laboratory, Golden, Colorado 80401, USA*  
(Dated: April 25, 2011)

We studied the general chemical trends of defect formation in MgTe using first-principles band structure methods. The formation energies and transition energy levels of intrinsic defects and extrinsic impurities and some defect complexes in zinc-blende MgTe were calculated systematically using a new hybrid scheme. The limiting factors for  $p$ -type and  $n$ -type doping in MgTe were investigated. Possible solutions to overcome the doping limitation of MgTe are proposed. The best  $p$ -type dopant is suggested to be N with nonequilibrium growth process and the best  $n$ -type dopant is suggested to be I with its doping complex  $V_{Mg}+4I_{Te}$ .

PACS numbers: 61.72.Bb, 61.72.uj, 71.23.An, 71.55.Gs

## I. INTRODUCTION

MgTe is a wide gap semiconductor which can exist either in NiAs or zincblende structure. Its ternary zinc-blende alloys such as MgCdTe and MgZnTe have been considered as potential candidates for low-cost, high efficiency, multi-junction thin film solar cell materials to complement existing CdTe and Cu(In,Ga)Se<sub>2</sub> solar materials<sup>1-3</sup>. The use of these alloys for high efficiency solid-state light-emission devices has also attracted much attention<sup>4-6</sup>. However, to be successful in these optoelectronic device applications, it is important to understand the defect properties of MgTe and its alloys because all these applications require that these alloys can be doped so sufficiently that carriers can be introduced at working temperature<sup>7-9</sup>. For CdTe, theoretical study has been systematically carried out to study its defect properties<sup>10</sup>. Based on the theoretical study, solutions to improve both  $n$ -type and  $p$ -type doping have been proposed. For MgTe, studies on DX centers and AX centers have been done in the past<sup>16,17</sup> and nitrogen doping was also investigated in MgTe-related alloys<sup>19</sup>. However, there is still no systematic theoretical study on its doping properties. Because of the large band gap of MgTe (3.49 eV) compared with that of CdTe (1.59 eV) and the different band alignment between CdTe and MgTe<sup>11</sup>, we expect that its defect properties of MgTe will be quite different from that of CdTe, which is the only II-VI semiconductor that can be relatively easily doped both  $n$ -type and  $p$ -type.

In this work, using first-principles band structure methods, we have systematically calculated the formation energies and transition energy levels of intrinsic defects and extrinsic impurities. Some defect complexes were also studied. Our calculations show that for  $p$ -type doping in MgTe, one of the limiting factors is not having a dopant with both high solubility and shallow acceptor levels: MgTe:N and MgTe:P have relatively shallow acceptor levels but high formation energies. P doping

in MgTe is also limited by the formation of AX centers. Moreover,  $p$ -type doping in MgTe is also limited by the spontaneous formation of compensating defects. When the Fermi energy is close to the VBM, the intrinsic donor defect  $Mg_i^{2+}$  can form spontaneously at the Mg-rich condition, thus limiting the  $p$ -type doping process. For the cases of MgTe:Na and MgTe:Cu, the doping process is also limited by the formation of compensating interstitial defects  $Na_i$  and  $Cu_i$ . The  $n$ -type doping is mainly limited by the spontaneous formation of intrinsic compensating defect  $V_{Mg}^{2-}$ . Another limiting factor is that most of the donor levels are too deep except for MgTe:I. Besides, DX centers are also found to spontaneously form in most of the  $n$ -type doping cases. To see if the defect complexes can improve the doping properties, we have also studied some defect complexes. However, we find that for  $p$ -type doping, the defect complexes in general do not lower the defect ionization energies. For  $n$ -type doping, the defect complexes can reduce the donor transition levels to some extent. Based on our study, we proposed that the best  $p$ -type dopant should be N incorporated using nonequilibrium growth process and the best  $n$ -type dopant is I and its complex with  $V_{Mg}$ .

## II. CALCULATION METHODS

Calculations were performed using the first-principles density functional theory<sup>20,21</sup> (DFT) based on local density approximation<sup>22</sup> (LDA), as implemented in the VASP code<sup>23,24</sup>. The electron and core interactions are included using the frozen-core projected augmented wave (PAW) approach<sup>25</sup>. The cut-off kinetic energy for the plane wave basis wave functions is chosen to be 300 eV for all the calculations. For pure zinc-blende MgTe, the lattice constant and bulk modulus are 6.380 Å and 390 kbar, respectively, in good agreement with experimental values of 6.414 Å and 376 kbar<sup>26</sup>. The calculated band gap at the theoretical lattice constant is 2.38 eV, 1.11 eV

less than the experimental value of 3.49 eV, typical in LDA calculations.

A defect or defect complex is modeled by putting the defect at or near the center of a periodic supercell. All the calculations are performed with a 64 atom supercell using  $4 \times 4 \times 4$  Monkhorst-Pack special  $k$ -point meshes<sup>27</sup>. In some cases, dense  $k$ -point meshes are used to check the convergence. For a charged defect, a uniform background charge is added to keep the global charge neutrality of the periodic supercell. All the internal structural parameters of the supercell are optimized by minimizing the total energy and quantum mechanical forces until the Hellman-Feynman forces acting on every atom become less than 0.01 eV.

To determine the defect formation energies and defect transition energy levels, we calculated the total energy  $E(\alpha, q)$  for a supercell containing the relaxed defect  $\alpha$  in its charge state  $q$ . We also calculated the total energy  $E(\text{MgTe})$  for the same supercell in the absence of the defect, as well as the total energies of elemental solids or gases at their stable phases. The defect formation energy  $\Delta H_f(\alpha, q)$  as a function of the electron Fermi energy<sup>28</sup>  $E_F$  as well as the atomic chemical potentials<sup>29,30</sup>  $\mu_i$  is as follows:

$$\Delta H_f(\alpha, q) = \Delta E(\alpha, q) + \sum n_i \mu_i + q E_F \quad (1)$$

where  $\Delta E(\alpha, q) = E(\alpha, q) - E(\text{MgTe}) + \sum n_i E(i) + q E_{VBM}$ .  $E_F$  is referenced to the valence band maximum (VBM) of MgTe.  $\mu_i$  is the chemical potential of constituent  $i$  referenced to elemental solid or gas with energy  $E(i)$ . The  $n$ 's are the number of Mg, Te, and extrinsic defect, and  $q$  is the number of electrons transferred from the supercell to the reservoirs in forming the defect cell. The defect transition energy level  $\epsilon_\alpha(q/q')$  is the Fermi energy  $E_F$  in Eq. (1) at which the formation energy  $\Delta H_f(\alpha, q)$  of defect  $\alpha$  and charge  $q$  is equal to that of another charge  $q'$  of the same defect, i.e.,

$$\epsilon_\alpha(q/q') = [\Delta E(\alpha, q) - \Delta E(\alpha, q')] / (q' - q) \quad (2)$$

To get fast convergence on total energy and transition energy levels and good descriptions on the symmetry of the defect state, a mixed scheme<sup>31,32</sup> was used. In this scheme, for an acceptor ( $q < 0$ ), the ionization energy level with respect to the VBM is given by:

$$\epsilon(0/q) = [\epsilon_D^\Gamma(0) - \epsilon_{VBM}^\Gamma(\text{MgTe})] + [E(\alpha, q) - (E(\alpha, 0) - q\epsilon_D^k(0))] / (-q) \quad (3)$$

For donor levels ( $q > 0$ ), the ionization energy referenced to the conduction band minimum (CBM) is given by:

$$\epsilon_g^\Gamma(\text{MgTe}) - \epsilon(0/q) = [\epsilon_{CBM}^\Gamma(\text{MgTe}) - \epsilon_D^\Gamma(0)] + [E(\alpha, q) - (E(\alpha, 0) - q\epsilon_D^k(0))] / q \quad (4)$$

where  $\epsilon_D^k(0)$  and  $\epsilon_D^\Gamma(0)$  are the defect levels at the special  $k$  points (averaged) and at the  $\Gamma$ -point, respectively; and  $\epsilon_{VBM}^\Gamma(\text{MgTe})$  and  $\epsilon_{CBM}^\Gamma(\text{MgTe})$  are the VBM and

CBM energy, respectively, of the pure MgTe supercell at the  $\Gamma$ -point. The first term on the right-hand side of Eq. (3) gives the single-electron defect level at the  $\Gamma$ -point. The second term determines the  $U$  energy parameter (including both the Coulomb contribution and atomic relaxation contribution) of the charged defect calculated at the special  $k$  points, which is the extra cost of energy after moving  $(-q)$  charge to the neutral defect level with  $E = \epsilon_D^k(0)$ . The formation energy of a charged defect is then given by:

$$\Delta H_f(\alpha, q) = \Delta H_f(\alpha, 0) - q\epsilon(0/q) + q E_F \quad (5)$$

where  $\Delta H_f(\alpha, 0)$  is the formation energy of the charge-neutral defect and  $E_F$  is the Fermi level with respect to the VBM. This approach has been used successfully for studying defects in various semiconductors.

### III. ORIGINS OF DOPING LIMITS

Generally speaking, three main factors could cause the doping limits: (i) the formation energies of desirable dopants are relatively large, thus limiting their solubility; (ii) the desirable dopants have sufficient solubility, but they produce deep levels, which are not ionized at working temperatures; and (iii) their compensating defects could form spontaneously, stopping the doping process or changing the doping type, like forming AX and DX centers<sup>15-18</sup>. The first factor depends highly on the selected dopants and growth conditions. The second factor only depends on the selected dopants. These two factors can be suppressed by selecting appropriate dopants and controlling the growth conditions. The third factor is an intrinsic problem for semiconductors and usually very difficult to overcome. We will discuss these factors one by one in detail and try to understand the doping properties of MgTe in the following sections.

### IV. FORMATION ENERGIES OF THE NEUTRAL POINT DEFECTS

Table I shows the calculated formation energies  $\Delta H_f(\alpha, 0)$  of neutral tetrahedrally coordinated point defects at  $\mu_i = 0$ , from which we can deduce the defect formation energies at different chemical potentials through Eq. (1). The non-tetrahedrally coordinated point defects such as AX and DX centers will be analyzed later in this paper. For donors, the difference between the calculated gap and the experimental gap multiplying the number of electrons at the donor level has been added to the formation energies. We notice that there are two interstitial sites in the zinc-blende structure, one site is surrounded by anions (a) and the other is surrounded by cations (c). For charge neutral Te, Mg, and Na interstitial, we find that the cation site has lower formation energies than the anion site. For charge neutral Cu interstitial, the anion site has a slightly lower formation energy. However, when

TABLE I: The formation energies  $\Delta E(\alpha, 0)$  of neutral tetrahedrally coordinated point defects at  $\mu_i = 0$ . For donors, the formation energies have been corrected by adding the difference between the calculated gap and the experimental gap multiplied by the number of electrons on the donor levels.

Defect	$\Delta E(\alpha, 0)$ (eV)	$\Delta E(\alpha, 0)$ (eV)	
$V_{Mg}$	4.30	$Mg_{Te}$	7.70
$V_{Te}$	5.89	$Te_{Mg}$	6.48
$Te_i^a$	3.33	$Mg_i^a$	4.85
$Te_i^c$	2.94	$Mg_i^c$	4.34
$Na_{Mg}$	1.63	$Al_{Mg}$	2.95
$Cu_{Mg}$	2.73	$Ga_{Mg}$	3.13
$Ag_{Mg}$	2.68	$In_{Mg}$	3.18
$Au_{Mg}$	2.82	$F_{Te}$	-2.21
$N_{Te}$	2.07	$Cl_{Te}$	1.61
$P_{Te}$	1.94	$Br_{Te}$	1.86
$As_{Te}$	1.95	$I_{Te}$	2.31
$Sb_{Te}$	2.42	$Cu_i^a$	3.46
$Bi_{Te}$	2.92	$Cu_i^c$	3.48
$Na_i^a$	2.04	$Na_i^c$	1.95

these defects are charged, the order could be reversed for intrinsic defects. This will be seen later in this paper. From this table, we can see that the formation energies of charge neutral intrinsic defects are relatively large.

## V. THE EFFECT OF CHEMICAL POTENTIALS

From Table I and Eq. (1), we can derive the defect formation energies, and consequently, the solubility of the dopants, as a function of the atomic chemical potentials. Therefore, theoretically, we can control the dopant solubility by adjusting the chemical potential of the dopant. However, there are some thermodynamic limits on the achievable values of the chemical potentials  $\mu_i$  under equilibrium growth conditions. First, the precipitation of Mg, Te, and the elemental dopant  $A$  ( $A = Na, Cu, In, Cl$ , etc.) should be avoided, which demands

$$\mu_{Mg} \leq 0, \mu_{Te} \leq 0, \mu_A \leq 0 \quad (6)$$

Secondly, the compound  $MgTe$  should maintain stable, so

$$\mu_{Mg} + \mu_{Te} = \Delta H_f(MgTe) \quad (7)$$

where  $\Delta H_f(MgTe)$  is the formation energy of the solid  $MgTe$ . The calculated  $\Delta H_f(MgTe) = -2.09$  eV is in good agreement with the experimental value  $-2.18$  eV<sup>19</sup>. Finally, to avoid the formation of the secondary compounds between the dopants  $A$  and the host elements, it requires

$$n\mu_A + m\mu_{Mg} \leq \Delta H_f(Mg_mA_n) \quad (8)$$

or

$$n\mu_A + m\mu_{Te} \leq \Delta H_f(A_nTe_m) \quad (9)$$

For example, in the case of  $Na_{Mg}$ , to avoid the formation of  $Na_2Te$  (with a calculated formation energy of  $-2.98$  eV), the achievable  $\mu_{Na}$  at Mg-rich condition [ $\mu_{Mg} = 0, \mu_{Te} = \Delta H_f(MgTe) = -2.09$  eV] should be less than  $-0.45$  eV. At Te-rich condition ( $\mu_{Mg} = -2.09$  eV,  $\mu_{Te} = 0$ ),  $\mu_{Na}$  should be less than  $-1.47$  eV. Above these chemical potential limits, secondary  $Na_2Te$  compound will form and the doping process is limited. Another example is the codoping of  $2Cu_{Mg} + Cl_{Te}$ . In this case, the chemical potentials of Cu, Cl, Mg, and Te are limited by the formation of  $CuCl$ ,  $MgCl_2$ , and  $Cu_2Te$ . The calculated formation energies of  $CuCl$  and  $MgCl_2$  are  $-1.12$  and  $-6.35$  eV and the formation energy of  $Cu_2Te$  is almost zero. So the highest possible Cl chemical potential is  $-2.13$  eV at Mg-poor condition. This indicates that the formation of  $Cl_{Te}$  will be not easy. Possible proposed solutions to overcome the solubility problem include increasing the dopant chemical potential through non-equilibrium process such as epitaxial growth<sup>33</sup> and using metastable compounds such as  $NaTe$ ,  $CuTe$ , or plasma sources<sup>34</sup> in which Na and Cu have higher chemical potentials. In general, it is necessary to consider all the chemical potential limits in searching for the lowest possible formation energy of a defect or defect complex and one may have to go beyond thermodynamic equilibrium to enhance dopant solubility.

## VI. SINGLE-ELECTRON LEVELS OF INTRINSIC DEFECTS AT $\Gamma$ -POINT

For intrinsic defects, due to sometimes large perturbation, it is not always easy to say whether a defect is an acceptor or a donor. It depends on the position of the defect electron energy level. Figure 1 shows the single-electron energy levels of tetrahedrally coordinated charge neutral intrinsic defects. Generally speaking, if a low-valence atom substitutes a high-valence atom (e.g.,  $Mg_{Te}$ ) or the site becomes a vacancy ( $V_{Mg}$ ), the defect states can be considered as created from the host valence ( $v$ ) band states that move upward in energy and consist of a low-lying singlet  $a_1^v$  state and a high-lying threefold-degenerate  $t_2^v$  state. If a low-valence atom is replaced by a high-valence atom (e.g.,  $Te_{Mg}$ ) or if a dopant goes to an interstitial site (e.g.,  $Cd_i$  and  $Te_i$ ), the defect states  $a_1^v$  and  $t_2^v$  will remain inside the valence band while the  $a_1^c$  and  $t_2^c$  states are created from the host conduction ( $c$ ) band states that move downward in energy. These states are occupied by the nominal valence electrons of the defect plus the valence electrons associated with the neighboring atoms and their positions depend on the potential difference between the dopant and host element and decide whether the defect is an acceptor or a donor. For example, for charge neutral  $V_{Mg}$ , the defect center has a total of  $0 + 6 = 6$  electrons. Two of them will occupy the  $a_1^v$  state and the remaining four electrons will occupy the  $t_2^v$  states just above the VBM, so  $V_{Mg}$  is an acceptor. For charge neutral  $V_{Te}$ , there are  $0 + 2 = 2$

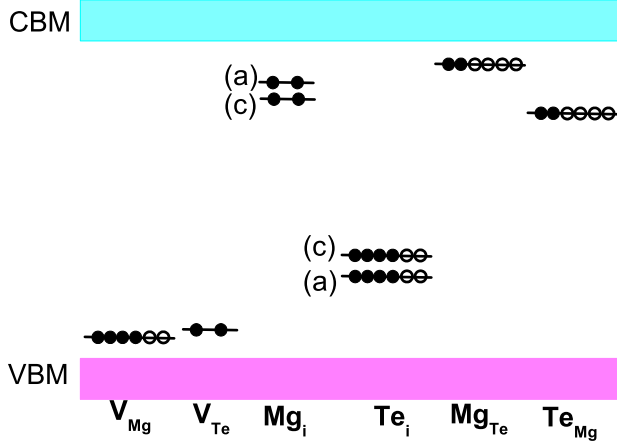


FIG. 1: (Color on line) Calculated single-electron defect levels for the tetrahedrally coordinated charge neutral intrinsic defects. The solid dots and the open dots give the occupation of the states.

electrons associated with the defect center and they will fully occupy  $a_1$  Mg dangling bond state, which is found to be above VBM. Because the  $a_1$  state is fully occupied and the  $t_2$  dangling bond states are found to be above CBM,  $V_{Te}$  can only be a donor. For the antisite defect  $Mg_{Te}$ , the defect center has  $2 + 2 = 4$  electrons. Two of them occupy the  $a_1^v$  state and the other two occupy the  $t_2^v$  states. The partially occupied  $t_2^v$  states move up and become close to the CBM due to the large electronegativity difference between Mg and Te, so  $Mg_{Te}$  is a donor. For  $Te_{Mg}$ , there are  $6 + 6 = 12$  electrons associated with the defect center. Eight of them will fill  $a_1^v$  and  $t_2^v$  states, two will fill  $a_1^c$  state, and the remaining two will occupy the  $t_2^c$  states. The partially occupied  $t_2^c$  states are close to the CBM, so  $Te_{Mg}$  is also a donor. For the interstitial defect  $Mg_i$ , two electrons will fully occupy the  $a_1^c$  state and is expected to be a donor.  $Te_i$  has six electrons and two of them will fill  $a_1^c$  state while the remaining four electrons will occupy the  $t_2^c$  states. Because the partially occupied  $t_2^c$  states are close to the VBM,  $Te_i$  is expected to be a deep acceptor. Figure 1 shows that the state of  $Mg_i^a$  is higher in energy than that of  $Mg_i^c$ . Table I also shows for charge neutral Mg interstitial, the anion site has a higher formation energy. However, when removing two electrons from the defect state and the defect becomes doubly charged  $Mg_i^{2+}$ , we find that the order is reversed and  $Mg_i^a$  has a lower formation energy. This is because the energy gain in  $Mg_i^a$  is more than that in  $Mg_i^c$  during the process of electron-removing. Similar situation happens in  $Te_i$  and the order is also reversed. This illustrates that the stable position of a defect could depend sensitively on its charge state.

## VII. DOPANTS SELECTION

For intrinsic defects, we can estimate whether they are acceptors or donors through the analysis above. For simple extrinsic impurities, by counting the number of the valence electrons of the dopants and the host elements, we can easily predict whether a dopant is a donor with a single-electron energy state close to the CBM or an acceptor with a single-electron energy state close to the VBM. For example, we can expect that group-*I* elements substituting on the Mg site  $X_{Mg}^I$  ( $X^I = \text{Na, Cu, Ag, and Au}$ ) or group-*V* elements substituting on the Te site  $Y_{Te}^V$  ( $Y^V = \text{N, P, As, Sb, and Bi}$ ) give acceptors, whereas group-*III* elements substituting on the Mg site  $X_{Mg}^{III}$  ( $X^{III} = \text{Al, Ga, and In}$ ) or group-*VII* elements substituting on the Te site  $Y_{Te}^{VII}$  ( $Y^{VII} = \text{F, Cl, Br, and I}$ ) or group-*I* interstitial ( $Cu_i$  and  $Na_i$ ) give donors.

Figure 2 shows our calculated acceptor transition energy levels using Eq. (3) and Figure 3 gives the donor transition energy levels calculated through Eq. (4). Using the charge neutral formation energies in Table I and these data, we can get the formation energies of charged defects as a function of the Fermi energy and chemical potentials using Eq. (5). A good dopant is expected to have a relatively shallow transition energy level.

### A. Acceptor Selection

Figure 2 shows the acceptor transition energy levels. For  $Te_i$ , its transition energy levels (0/-) and (-/2-) are at 0.80 and 0.84 eV above the VBM. For  $V_{Mg}$ , its transition energy levels (0/-) and (-/2-) are at 0.28 and 0.39 eV above the VBM. Because their transition energy levels are too high, neither  $Te_i$  nor  $V_{Mg}$  is a good intrinsic acceptor for  $MgTe$ .

For  $X_{Mg}^I$ , where  $X = \text{Cu, Ag, and Au}$ , the calculated (0/-) transition energy levels are at 0.41, 0.31, and 0.47 eV above the VBM, respectively. Because group-*IB*  $d$  orbitals couple strongly to Te  $p$  orbitals, these transition energy levels are relatively deep. As Ag has the lowest  $d$  orbital energy and the largest atomic size, the  $p-d$  repulsion is the weakest among the three group-*IB* atoms. This can explain why  $Ag_{Mg}$  has a shallower (0/-) transition energy level than  $Cu_{Mg}$  and  $Au_{Mg}$ . If we further reduce  $p-d$  repulsion by replacing group-*IB* atoms with group-*IA* atoms, the transition energy levels should be further shallowed. Considering this, we find that the (0/-) level of  $Na_{Mg}$  is 0.10 eV above the VBM and it could be an important acceptor.

For  $Y_{Te}^V$ , where  $Y = \text{N, P, As, Sb, and Bi}$ , the calculated (0/-) transition energy levels are at 0.10, 0.12, 0.19, 0.42, and 0.60 eV above VBM, respectively. We can see the transition energy level increases as the atomic number of  $Y$  increases. This is because the defect level has strong  $Y^V$   $p$  character and as the atomic number increases, its  $p$  atomic orbital energy also increases, thus, increasing



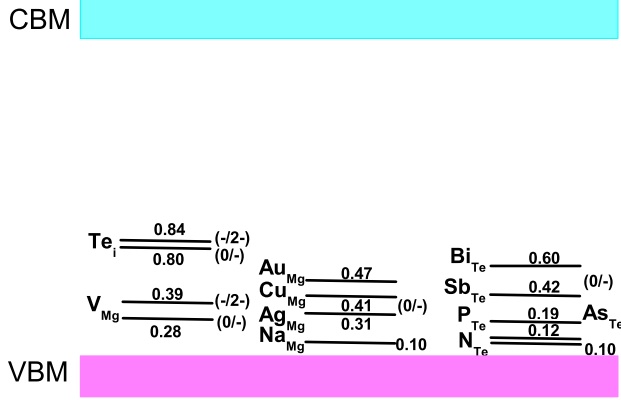


FIG. 2: (Color on line) Calculated acceptor transition energy levels for the tetrahedrally coordinated point defects.

the energy of defect state. From the data, we can see N and P could be important *p*-type dopants for MgTe. We also find that N induces a sizable lattice distortion because of its small ionic radius. The Mg-N bond length is about 27% shorter than a normal Mg-Te length, in good agreement with previous calculation<sup>16</sup>.

### B. Donor Selection

For most intrinsic donors, the transition energy levels are relatively deep, as shown in Figure 3. The shallowest level is  $\text{Mg}_{\text{Te}}$  (2+/0) transition energy level, which is 0.19 eV below the CBM. However, the formation energy of  $\text{Mg}_{\text{Te}}$  is really large, as shown in Table I, so this intrinsic defect is not a good donor.  $\text{Mg}_{\text{Te}}$ ,  $\text{Mg}_i$ , and  $\text{V}_{\text{Te}}$  are all found to be negative-U systems, i.e., the  $q=+1$  charged states are unstable with respect to dissociating into the  $q=+2$  and  $q=0$  states.

For  $\text{X}_{\text{Mg}}^{\text{III}}$ , where X=Al, Ga, and In, the calculated (+/0) transition energy levels are at 0.19, 0.65, and 0.56 eV below the CBM, respectively. Because the defect state has mostly the cation *s* character and the Ga 4*s* orbital is lower in energy than the Al 3*s* and In 5*s* orbital,  $\text{Ga}_{\text{Mg}}$  has a deeper transition energy level than  $\text{Al}_{\text{Mg}}$  and  $\text{In}_{\text{Mg}}$ . Moreover, we find that these three defects are easy to form DX centers (see below). Because their transition energy levels are all relatively deep, they are not good *n*-type dopants.

For  $\text{Y}_{\text{Te}}^{\text{VII}}$ , where Y=F, Cl, Br, and I, the calculated (+/0) transition energy levels are at 0.92, 0.29, 0.21, and 0.06 eV below the CBM, respectively. Because the defect state has a largely anion *s* character and the *s* orbital of group-VII atom increases with the atomic number, the donor level gets shallower from F to Cl to Br to I. These data shows that I could be a good *n*-type dopant.

For  $\text{Cu}_i$  and  $\text{Na}_i$ , the calculated (+/0) transition energy levels are at 0.14 and 0.04 eV below the CBM. We

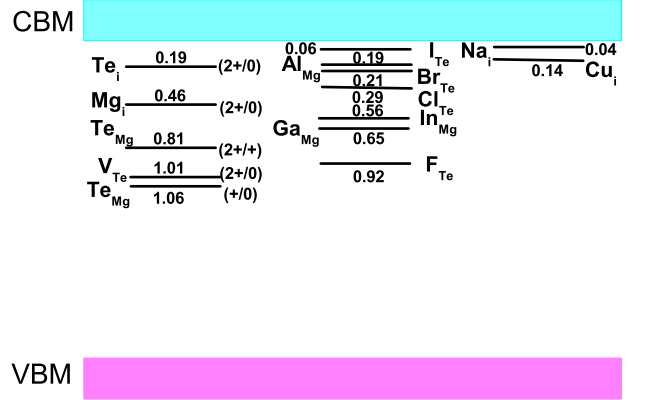


FIG. 3: (Color on line) Calculated donor transition energy levels for the tetrahedrally coordinated point defects.

can see  $\text{Na}_i$  could be a good *n*-type dopant but we also need to keep in mind that  $\text{Na}_{\text{Mg}}$  is also a relatively good *p*-type dopant. Similar case happens to  $\text{Cu}_i$ .

## VIII. COMPENSATION DEFECTS

Through the analysis above, we have already selected some candidate shallow acceptors and donors.  $\text{Na}_{\text{Mg}}$ ,  $\text{N}_{\text{Te}}$ , and  $\text{P}_{\text{Te}}$  could be good *p*-type dopants while  $\text{I}_{\text{Te}}$ ,  $\text{Na}_i$  and  $\text{Cu}_i$  could be good candidates for *n*-type doping. None of the intrinsic defects are good for either *p*-type or *n*-type doping of MgTe. However, as an intrinsic problem for semiconductors, compensating defects could form spontaneously, thus limiting the doping process or changing the doping type. These compensation defects include intrinsic compensation defects, impurity self-compensation defects, AX centers and DX centers, etc.. We will discuss each of these factors as follows.

### A. Intrinsic compensation defects

The calculated formation energies of intrinsic defects as a function of the Fermi energy are shown in Figure 4, where the slope of the energy line gives the charge state of a defect at that  $E_F$  and the inflexions are calculated transition energy levels. From this Figure, we can see that for undoped MgTe, at Mg-rich condition,  $E_F$  tends to be near the middle of the gap. This is because if  $E_F$  is below the mid-gap, the compensating donor defect  $\text{Mg}_i^{2+}$  will easily form, thus pushing  $E_F$  upward. On the other hand, if  $E_F$  is above the mid-gap, the compensating acceptor defect  $\text{V}_{\text{Mg}}^{2-}$  will become the dominant intrinsic defect and pull  $E_F$  downward. Thus, the Fermi energy will more or less be pinned in the middle of the band gap. Similarly, at Te-rich limit,  $E_F$  tends to be pinned more close to the VBM for undoped MgTe and makes MgTe

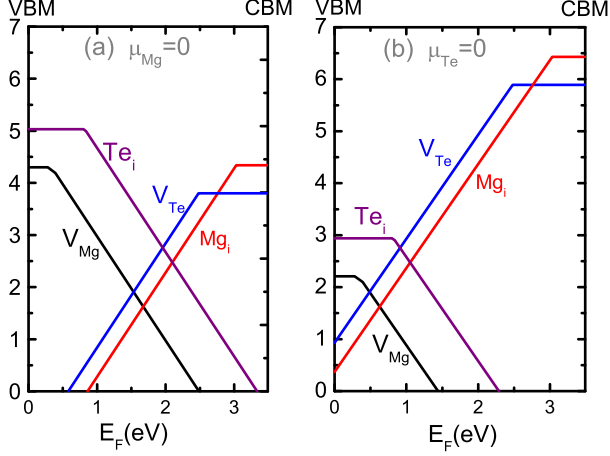


FIG. 4: (Color on line) Calculated formation energies of intrinsic defects as a function of Fermi levels at (a) Mg-rich condition and (b) Te-rich condition, respectively.

*p*-type. Through the analysis, we could expect undoped MgTe to be either semi-insulating or slightly *p*-type under equilibrium growth condition.

We also need to notice that at Mg-rich condition, when  $E_F$  is close to the VBM, the defect  $\text{Mg}_i^{2+}$  can form spontaneously. Therefore, if we want to get *p*-type MgTe, the growth should be carried out under Te-rich limit. At this condition, we can expect that  $\text{Y}_{\text{Te}}^V$  will have the highest formation energies, thus limiting the solubility of group-V elements in MgTe. For  $\text{N}_{\text{Te}}$  and  $\text{P}_{\text{Te}}$ , considering the formation energies of  $\text{Mg}_3\text{N}_2$  (-3.35 eV) and  $\text{Mg}_3\text{P}_2$  (-3.81 eV), the lowest possible formation energies are 2.07 and 1.94 eV, respectively, at Te-rich limit using equilibrium growth process. Although they have shallow acceptor levels, they are still not good acceptors except we can increase their solubility, which might be carried out using non-equilibrium growth process. For  $\text{Na}_{\text{Mg}}$ , at Te-rich condition, it will have the lowest formation energy. However, it's still not a good acceptor due to impurity self-compensation, as we will see below.

When  $E_F$  is close to the CBM, the defect  $\text{V}_{\text{Mg}}^{2-}$  can form spontaneously whether Mg is rich or Te is rich. This is an intrinsic limit on the possible *n*-doping in MgTe and explains why MgTe is very difficult to be doped *n*-type.

### B. Impurity self-compensation defects

Impurity self-compensation might happen for impurity doping and will limit the doping process. As we have mentioned above,  $\text{Na}_{\text{Mg}}$  might be a good acceptor. However, we should also remember  $\text{Na}_i$  might be a good

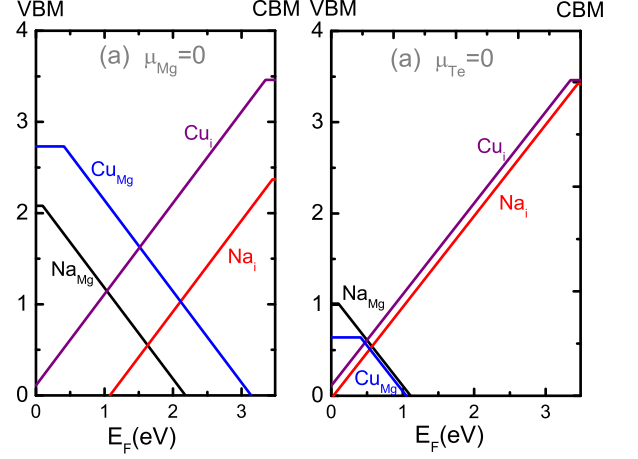


FIG. 5: (Color on line) Calculated formation energies of  $\text{Na}_i$ ,  $\text{Na}_{\text{Mg}}$ ,  $\text{Cu}_i$ , and  $\text{Cu}_{\text{Mg}}$  as a function of Fermi levels at (a) Mg-rich condition and (b) Te-rich condition, respectively.

donor. Figure 5 shows the formation energies of  $\text{Na}_{\text{Mg}}$ ,  $\text{Na}_i$ ,  $\text{Cu}_{\text{Mg}}$ , and  $\text{Cu}_i$  as a function of the Fermi energy at the Mg-rich and Te-rich conditions, respectively. We can see that Na is not a good dopant. This is because if  $\text{Na}_{\text{Mg}}$  is used as an acceptor, the Fermi energy level will be lowered as the concentration of  $\text{Na}_{\text{Mg}}$  increases and the defect  $\text{Na}_i^+$  becomes more stable. Thus, more and more Na will move to the interstitial site, compensating the *p*-type dopant  $\text{Na}_{\text{Mg}}$ . This occurs under both the Mg-rich and Te-rich conditions. This self-compensation effectively changes the shallow  $\text{Na}_{\text{Mg}}$  (0/-) transition energy level and the shallow  $\text{Na}_i$  (+/0) transition energy level to a deep negative  $U[\text{Na}_{\text{Mg}}(-)/\text{Na}_i(+)]$  transition. Similar situation happens for Cu doping.

### C. AX centers

In MgTe, *p*-type doping can also be limited by the formation of AX centers. The AX center forms through a double bond breaking (DBB) mechanism<sup>17,18</sup>, where two next neighbor anions move towards each other, breaking two neighboring anion-cation bonds and forming an anion-anion bond, as shown in Figure 6. If the defect states  $t_2^v$  have two holes, the DBB-like lattice distortion might break the local  $T_d$  symmetry into  $C_{2v}$ , moving the  $a_1$  state up and the  $e$  state down, thus lowering the electronic energy, as shown in Figure 6(c). If the energy gain by forming a new anion-anion bond is larger than the energy increase caused by breaking two cation-anion bonds, the AX center might become a stable state. However, in this case, a negatively charged shallow acceptor

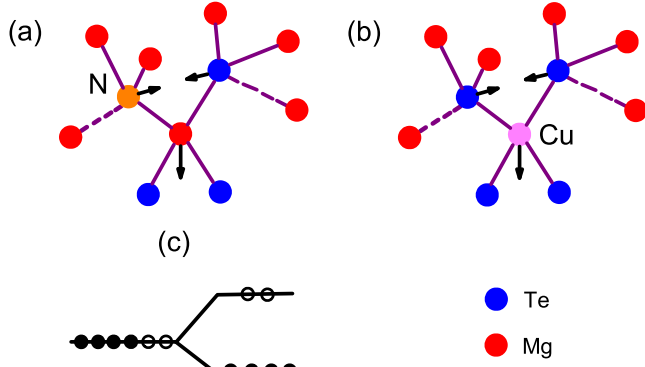


FIG. 6: (Color on line) A schematic plot of the double bond breaking (DBB) model of the AX center for (a) anion substitutional defect and (b) cation substitutional defect. Panel (c) shows schematically how the AX center can be stabilized by lowering the electronic energy.

can be converted to be a positively charged deep donor, thus limiting the doping process. To see whether AX centers are stable in MgTe, we calculated the AX formation energy defined as the energy difference

$$\Delta E(AX) = E(AX, q) - E(\alpha, q), \quad (10)$$

where  $E(AX, q)$  is the total energy of an AX center with charge state  $q$  and  $E(\alpha, q)$  is the total energy of the corresponding tetrahedrally coordinated defect  $\alpha$  at the same charge state  $q$ . Our calculated results show that for  $N_{Te}^+$ ,  $P_{Te}^+$ ,  $As_{Te}^+$ , and  $Sb_{Te}^+$ ,  $\Delta E(AX)$  are 0.51, -0.23, -0.29, and -0.35 eV with the dopant-Te bond lengths 2.17, 2.60, 2.71, and 2.89 Å at the AX center state, respectively. These results show that for N doping, the AX center is unstable, thus does not limit the doping process. This is different from Chadi's work<sup>17</sup>, where he found N doped MgTe was stable at the AX center state with a formation energy of -0.30 eV. However, for other group-V elements doping, AX centers might be a limiting factor as they are more stable. Thus, although  $P_{Te}$  creates relatively shallow acceptor level when P is tetrahedrally coordinated, it's not a good  $p$ -type dopant for MgTe because the effective negative- $U$  ( $\alpha^-/AX^+$ ) transition energy level is deeper. We also calculated  $\Delta E(AX)$  of  $Cu_{Mg}^+$  and  $Ag_{Mg}^+$  and the results are 0.34 and 0.35 eV, respectively. This indicates AX centers are not limiting factors for the doping of Cu and Ag, but the deep transition energy levels and impurity self-compensations are.

#### D. The DX centers

In MgTe, except by the intrinsic defect  $V_{Mg}^{2-}$ ,  $n$ -type doping can also be limited by DX centers. The DX center forms through a single bond breaking (SBB) model<sup>15,16</sup>,

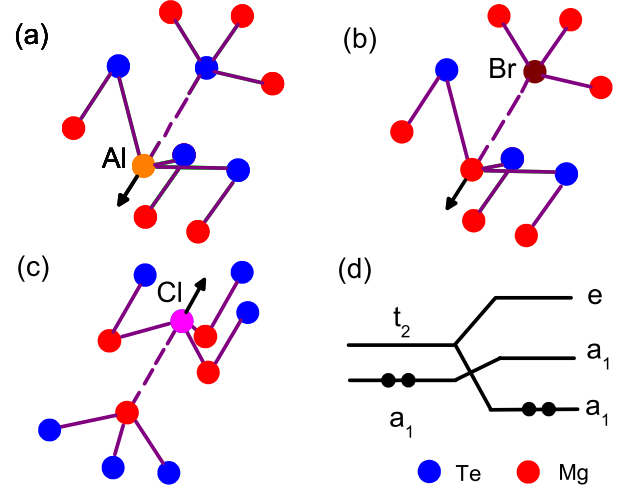


FIG. 7: (Color on line) A schematic plot of the single bond breaking (SBB) model of the DX center for (a) cation substitutional defect with cation displacement, (b) anion substitutional defect with cation displacement, and (c) anion substitutional defect with anion displacement. Panel (d) shows schematically how the DX center can be stabilized by lowering electronic energy.

where a cation-anion bond breaks along the  $\langle 111 \rangle$  direction, changing the local symmetry from  $T_d$  to  $C_{3v}$ . The defect states  $t_2^c$  will split into an  $a_1$  state and an  $e$  state. The  $a_1(t_2^c)$  will couple with  $a_1(a_1^c)$ , pushing one of them down, thus lowering the electronic energy as shown in Figure 7(d). If the energy gain is larger than the energy increase caused by breaking the one bond, the DX center becomes a stable state. In this case, a positively charged shallow donor can be converted to a negatively charged deep acceptor, thus limiting the doping process. To see whether DX centers are stable in MgTe, we calculated the DX formation energy defined as the energy difference

$$\Delta E(DX) = E(DX, q) - E(\alpha, q), \quad (11)$$

where  $E(DX, q)$  is the total energy of an DX center with charge state  $q$  and  $E(\alpha, q)$  is the total energy of the corresponding tetrahedrally coordinated defect  $\alpha$  at the same charge state  $q$ . We noticed that there are two cases of bond breaking along  $\langle -1, -1, -1 \rangle$  or  $\langle 111 \rangle$ . We considered these two DX states and defined our  $E(DX, q)$  as the energy of the state which has a smaller total energy. In the cases of  $Al_{Mg}^-$ ,  $Ga_{Mg}^-$ ,  $In_{Mg}^-$ ,  $Br_{Te}^-$ , and  $I_{Te}^-$ , the cations are displaced, while anions are displaced in the cases of  $F_{Te}^-$  and  $Cl_{Te}^-$ . We find that for  $Al_{Mg}^-$ ,  $Ga_{Mg}^-$ , and  $In_{Mg}^-$ ,  $\Delta E(DX)$  are -0.65, -0.32, and -0.39 eV, respectively, compared to Chadi's results<sup>16</sup> -0.08 and -0.05 eV for  $Al_{Mg}^-$  and  $Ga_{Mg}^-$ . This indicates DX centers are all stable for group-III elements, thus limiting the doping of the three elements. For group-VII ele-



ments,  $\Delta E(DX)$  are -0.52, -0.30, -0.15, and -0.34 eV for  $F_{Te}^-$ ,  $Cl_{Te}^-$ ,  $Br_{Te}^-$ , and  $I_{Te}^-$ , respectively. Thus the DX centers are also a limiting factor for the doping of group-VII elements.

## IX. THE DOPING COMPLEXES

From the above discussions, we can see that for most dopants, either  $n$ -type or  $p$ -type, the transition energy levels are relatively deep, thus limiting their doping abilities. One suggested solution is trying to form defect complexes to lower the transition levels through the coupling between the donor-acceptor states. We have tested this idea by studying some of the defect complexes. For the  $p$ -type complexes, we tested  $V_{Mg}+Cl_{Te}$ ,  $In_{Mg}+2Sb_{Te}$ ,  $2Cu_{Mg}+Cl_{Te}$ , and  $V_{Mg}+Cu_i$ . The calculated (0/-) transition energy levels are 0.39, 0.44, 0.43, and 0.27 eV above the VBM, respectively. Comparing to the corresponding point defects, we find these  $p$ -type complexes in general can't lower the defect ionization energies. For the  $n$ -type doping, we checked the complexes  $V_{Mg}+3I_{Te}$ ,  $V_{Mg}+3Br_{Te}$ . The calculated (+/0) transition energy levels are -0.09 and 0.16 eV, respectively, relative to the CBM. Also we find that for clusters  $V_{Mg}+4I_{Te}$  and  $V_{Mg}+4Br_{Te}$ , the (2+/0) transition energy levels are 0.07 and 0.19 eV below the CBM. For  $Cu_{Mg}+2Br_{Te}$ , our calculated (+/0) transition energy level is 0.15 eV below the CBM. In general, we find that the defect complexes can reduce the donor transition energy levels to some extent for MgTe at high dopant concentrations.

## X. CONCLUSIONS

The doping properties of MgTe have been systematically studied using first-principles band structure methods. The formation energies and transition energy levels of intrinsic defects and extrinsic impurities are calculated using a mixed scheme, as well as for some defect complexes. We show that for  $p$ -type doping in MgTe, it's difficult to find a dopant with both high solubility and a shallow accept level. This is the cases for MgTe:N and MgTe:P, which have relatively shallow acceptor levels but high formation energies. Another factor is the formation of AX centers, which happens to MgTe:P. Besides, it is also limited by the spontaneous formation of compensating defects. When the Fermi energy is close to the VBM, the intrinsic donor defect  $Mg_i^{2+}$  can form spontaneously at the Mg-rich condition, thus limiting the  $p$ -doping process. For the cases of MgTe:Na and MgTe:Cu, the doping process is also limited by the formation of the compensating interstitial defects  $Na_i$  and  $Cu_i$ . The  $n$ -type doping is mainly limited by the spontaneous formation of the intrinsic compensating defect  $V_{Mg}^{2-}$ . Another limiting factor is that most of the donor levels are too deep except for MgTe:I. Besides, the DX centers are also found to be stable when the Fermi energy is close to CBM in

all the studied  $n$ -type doping cases. Overall, our calculations suggest that the best  $p$ -type dopant should be N with a growth process incorporated by non-equilibrium technique and the best  $n$ -type dopant should be I and its defect complex  $V_{Mg}+4I_{Te}$  at high dopant concentration.

## XI. ACKNOWLEDGMENTS

The work at Fudan University is partially supported by the National Science Foundation of China, the Special Funds for Major State Basic Research, and the project of MOE and Shanghai Municipality. The computation is performed in the Supercomputer Center of Shanghai, the Supercomputer Center of Fudan University, and CCS. The work at NREL is funded by the U.S Department of Energy (DOE), under Contract No. DE-AC36-08GO28308.

- 
- <sup>1</sup> A. Shah, P. Torres, R. Tscharnner, N. Wyrsh, and H. Keppner, *Science* **285**, 692 (1999).
  - <sup>2</sup> L. L. Kazmerski, F. R. White, and G. K. Morgan, *Appl. Phys. Lett.* **29**, 268 (1976).
  - <sup>3</sup> K. Mitchell, A. L. Fahrenbruch, and R. H. Bube, *J. Vac. Sci. Technol.* **12**, 909 (1975).
  - <sup>4</sup> J.-H. Yang, S. Chen, W.-J. Yin, X. G. Gong, A. Walsh, and S.-H. Wei, *Phys. Rev. B* **79**, 245202 (2009).
  - <sup>5</sup> M. W. Wang, M. C. Phillips, J. F. Swenberg, E. T. Yu, J. O. McCaldin, and T. C. McGill, *J. Appl. Phys.* **73**, 4660 (1993).
  - <sup>6</sup> M. W. Wang, J. F. Swenberg, M. C. Phillips, E. T. Yu, J. O. McCaldin, R. W. Grant, and T. C. McGill, *Appl. Phys. Lett.* **64**, 3455 (1994).
  - <sup>7</sup> R. K. Watts, W. C. Holton, and M. de Wit, *Phys. Rev. B* **3**, 404 (1971).
  - <sup>8</sup> R. M. Park, M. B. Trofer, C. M. Rouleau, J. M. Depuydt, and M. A. Haase, *Appl. Phys. Lett.* **57**, 2127 (1990).
  - <sup>9</sup> M. A. Haase, J. Qiu, J. DePuydt, and H. Cheng, *Appl. Phys. Lett.* **59**, 1272 (1991).
  - <sup>10</sup> S.-H. Wei and S. B. Zhang, *Phys. Rev. B* **66**, 155211 (2002).
  - <sup>11</sup> Y.-H. Li, A. Walsh, S. Chen, W.-J. Yin, J.-H. Yang, J. Li, J. L. F. Da Silva, X. G. Gong, and S.-H. Wei, *Appl. Phys. Lett.* **94**, 212109 (2009).
  - <sup>12</sup> A. Tsukazaki, A. Ohtomo, T. Onuma, M. Ohtani, T. Makino, M. Sumiya, K. Ohtani, S. F. Chichibu, S. Fuke, Y. Segawa, H. Ohno, H. Koinuma, and M. Kawasaki, *Nature Mater.* **4**, 42 (2005).
  - <sup>13</sup> B. Tsukazaki, M. Kubota, A. Ohtomo, T. Onuma, K. Ohtani, H. Ohno, S. F. Chichibu, and M. Kawasaki, *Jpn. J. Appl. Phys.* **44**, L643 (2005).
  - <sup>14</sup> M. Joseph, H. Tabata, and T. Kawai, *Jpn. J. Appl. Phys.* **38**, L1205 (1999).
  - <sup>15</sup> D. J. Chadi and K. J. Chang, *Phys. Rev. Lett.* **61**, 873 (1988); *Phys. Rev. B* **39**, 10 063 (1989).
  - <sup>16</sup> D. J. Chadi, *Phys. Rev. Lett.* **72**, 534 (1994).
  - <sup>17</sup> C. H. Park and D. J. Chadi, *Phys. Rev. Lett.* **75**, 1134 (1995); *Phys. Rev. B* **55**, 12 995 (1997).
  - <sup>18</sup> D. J. Chadi, *Phys. Rev. B* **59**, 15 181 (1999).
  - <sup>19</sup> T. Baron, K. Saminadayar, S. Tatarenko, H. -J. Lugauer, A. Waag, and G. Landwehr, *J. Cryst. Growth* **184**, 415 (1998).
  - <sup>20</sup> P. Hohenberg and W. Kohn, *Phys. Rev.* **136**, B864 (1964).
  - <sup>21</sup> W. Kohn and L. J. Sham, *Phys. Rev.* **140**, A1133 (1965).
  - <sup>22</sup> D. M. Ceperley and B. J. Alder, *Phys. Rev. Lett.* **45**, 566 (1980).
  - <sup>23</sup> G. Kresse and J. Furthmüller, *Phys. Rev. B* **54**, 11169 (1996).
  - <sup>24</sup> G. Kresse and J. Furthmüller, *Comput. Mater. Sci.* **6**, 15 (1996).
  - <sup>25</sup> G. Kresse and D. Joubert, *Phys. Rev. B* **59**, 1758 (1999).
  - <sup>26</sup> O. M. Madelung, *Semiconductors: Data Handbook*, 3rd ed. (Springer, Berlin, 2004).
  - <sup>27</sup> H. J. Monkhorst and J. D. Pack, *Phys. Rev. B* **13**, 5188 (1976).
  - <sup>28</sup> G. A. Baraff and M. Schluter, *Phys. Rev. Lett.* **55**, 1327 (1985).
  - <sup>29</sup> S. B. Zhang and J. E. Northrup, *Phys. Rev. Lett.* **67**, 2339 (1991).
  - <sup>30</sup> D. B. Laks, C. G. Van de Walle, G. F. Neumark, P. E. Blochl, and S. T. Pantelides, *Phys. Rev. B* **45**, 10 965 (1992).
  - <sup>31</sup> S.-H. Wei, *Comput. Mater. Sci.* **30**, 337 (2004).
  - <sup>32</sup> Y. Yan and S.-H. Wei, *Phys. Stat. Sol.* **245**, 641 (2008).
  - <sup>33</sup> S. B. Zhang and S.-H. Wei, *Phys. Rev. Lett.* **86**, 1789 (2001).
  - <sup>34</sup> F. Fischer, A. Waag, G. Bilger, T. Litz, S. Scholl, M. Schmitt, and G. Landwehr, *J. Cryst. Growth* **141**, 93 (1994).